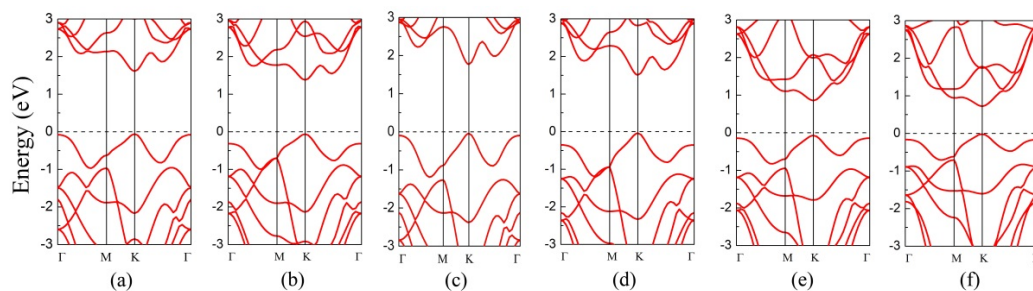
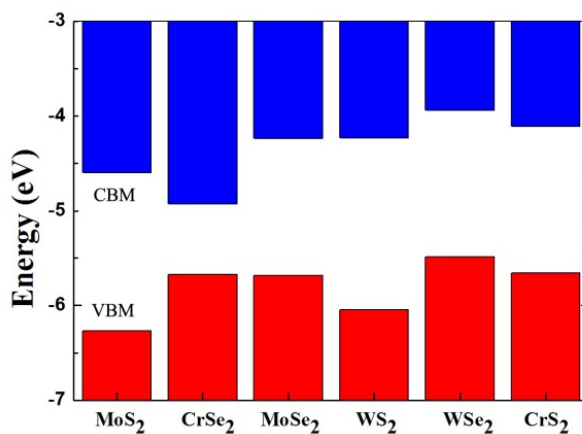


### Electronic Supplementary Information



**Figure S1.** Computed electronic band structures of (a) MoS<sub>2</sub>, (b) MoSe<sub>2</sub>, (c) WS<sub>2</sub>, (d) WSe<sub>2</sub>, (e) CrS<sub>2</sub>, and (f) CrSe<sub>2</sub> monolayer, based on PBE functional. All monolayers exhibits a direct bandgap.



**Figure S2.** Computed positions of CBM and VBM of TMD monolayers, respectively, using PBE functional. The vacuum level is set to zero.

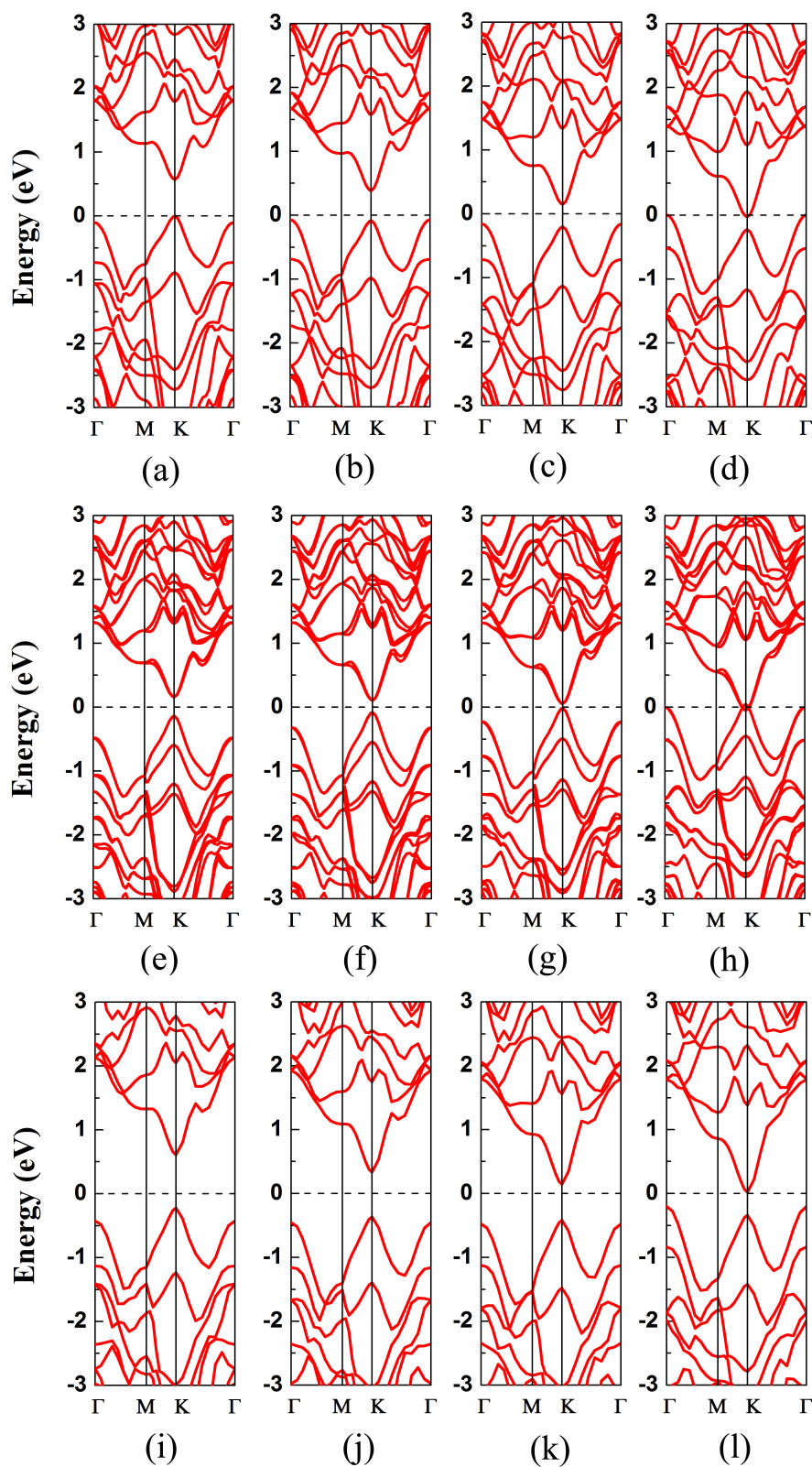


**Figure S3.** Computed electronic band structures (PBE) of  $\text{WSe}_2/\text{MoS}_2$  heterobilayer with (a) 0%, (b) 1%, (c) 2%, and (d) 4% biaxial strain. Computed band structure (PBE) of  $\text{WSe}_2/\text{MoS}_2$  with inclusion of spin-orbit coupling (SOC) effect and with (e) 0%, (f) 1%, (g) 2%, and (h) 4% biaxial strain. Computed band structures (**HSE06**) of  $\text{WSe}_2/\text{MoS}_2$  with (i) 0%, (j) 1%, (k) 2%, and (l) 4% biaxial strain.

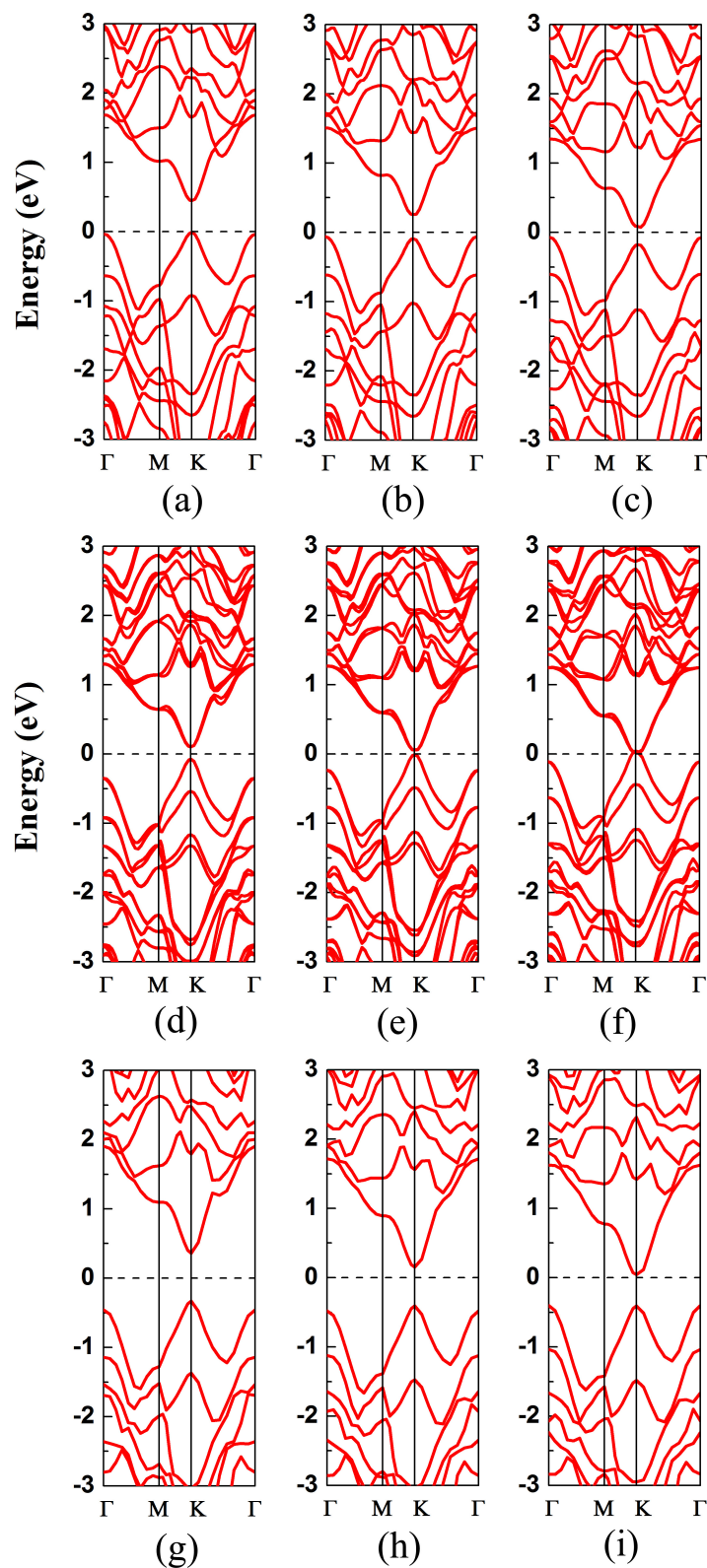


**Figure S4.** Computed electronic band structures (PBE) of WSe<sub>2</sub>/MoS<sub>2</sub> heterobilayer with (a) 2%, (b) 4%, and (c) 6% strain along the  $x$ -direction. Computed band structures of WSe<sub>2</sub>/MoS<sub>2</sub> with inclusion of SOC effect and with (d) 2%, (e) 4%, and (f) 6% strain along  $x$ -direction. Calculated band structures (HSE06) of WSe<sub>2</sub>/MoS<sub>2</sub> with (g) 2%, (h) 4%, and (i) 6% strain along  $x$ -direction.

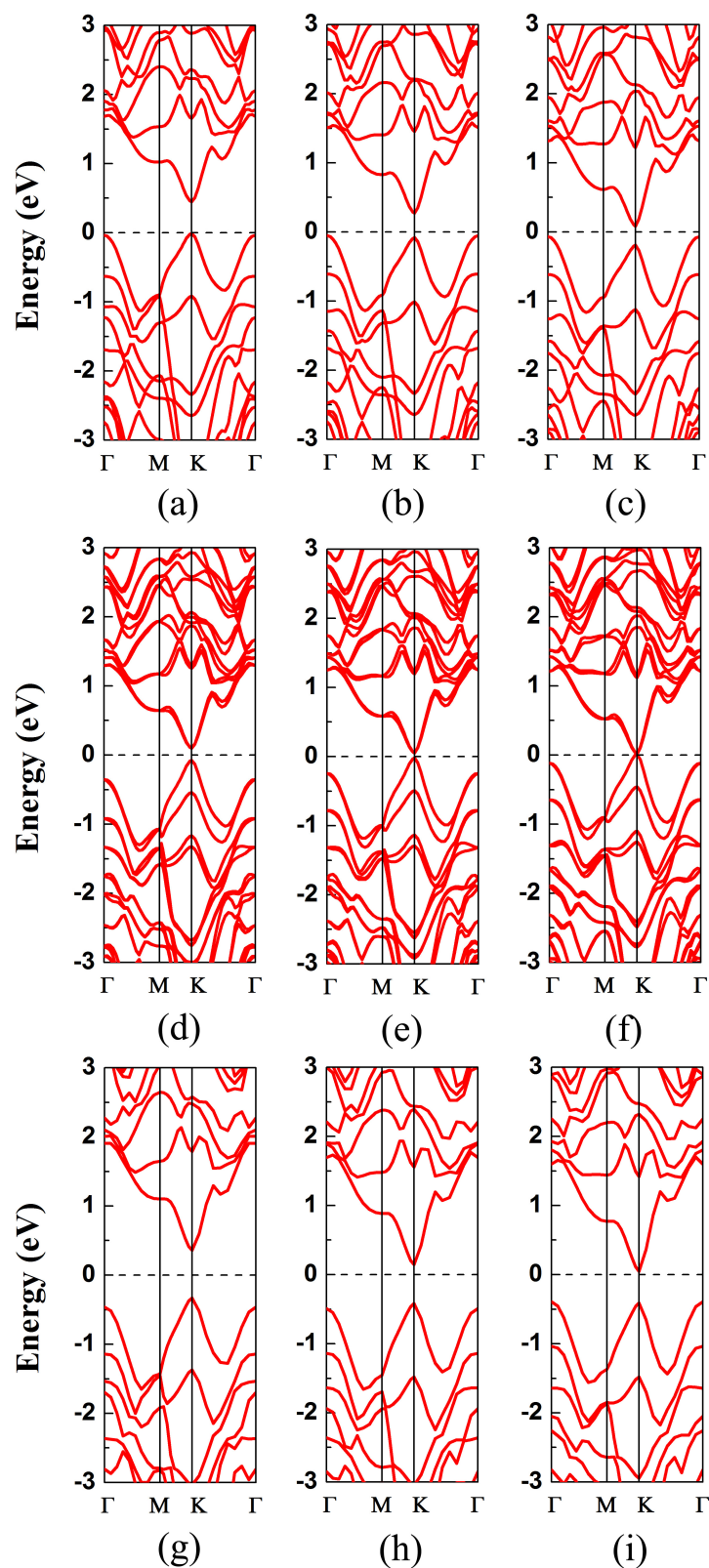


**Figure S5.** Computed electronic band structures (PBE) of WSe<sub>2</sub>/MoS<sub>2</sub> heterobilayer with (a) 2%, (b) 4%, and (c) 6% strain along the  $y$ -direction. Computed band structures of WSe<sub>2</sub>/MoS<sub>2</sub> with inclusion of SOC effect and with (d) 2%, (e) 4%, and (f) 6% strain along  $y$ -direction. Calculated band structures (HSE06) of WSe<sub>2</sub>/MoS<sub>2</sub> with (g) 2%, (h) 4%, and (i) 6% strain along  $y$ -direction.

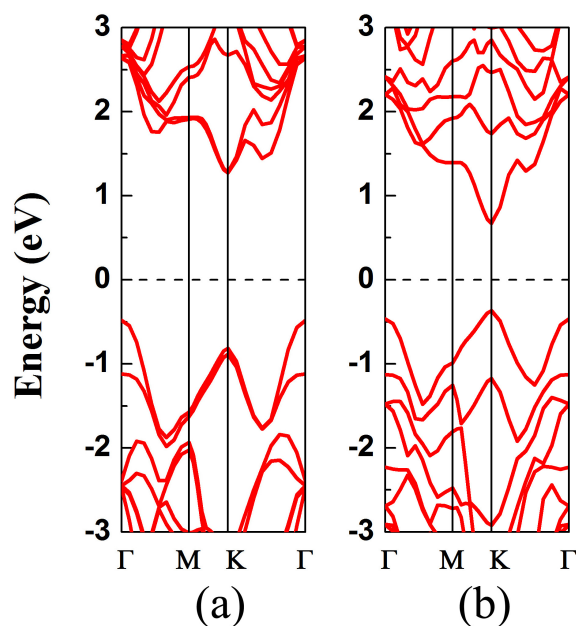


**Figure S6.** (a) Computed electronic band structures (HSE06) of MoS<sub>2</sub> bilayer. Note that the measured indirect bandgap of MoS<sub>2</sub> bilayer is about 1.53 eV (Ref. 25). So the computed HSE06 indirect bandgap (1.77 eV) overestimates the bandgap of MoS<sub>2</sub> bilayer. (b) Computed band structures (HSE06) of MoSe<sub>2</sub>/MoS<sub>2</sub> heterobilayer. The MoSe<sub>2</sub>/MoS<sub>2</sub> heterobilayer exhibits a direct bandgap. PBE calculation suggests MoSe<sub>2</sub>/MoS<sub>2</sub> heterobilayer possesses a quasi-direct bandgap (Figure 3(a)).

**Table S1.** Cell parameter  $a$  in Å and the distance  $d_{s-x}$  in Å between the two TMD heterobilayers.

Heterobilayer	$a$	$d_{s-x}$
MoSe <sub>2</sub> /MoS <sub>2</sub>	3.26	3.12
WS <sub>2</sub> /MoS <sub>2</sub>	3.19	3.10
WSe <sub>2</sub> /MoS <sub>2</sub>	3.26	3.11
CrS <sub>2</sub> /MoS <sub>2</sub>	3.13	3.18
CrSe <sub>2</sub> /MoS <sub>2</sub>	3.21	3.16
FeS <sub>2</sub> /MoS <sub>2</sub>	3.17	3.12
VS <sub>2</sub> /MoS <sub>2</sub>	3.19	3.08
VSe <sub>2</sub> /MoS <sub>2</sub>	3.26	3.14

**Table S2.** Computed Bader charge transfer between MoSe<sub>2</sub> and MoS<sub>2</sub> layer under different external electric field (normal to the plane of the bilayer).

Electric field (V/ Å)	0	0.1	0.2	0.3	0.4	0.5	0.6
Charge (e)	0.0099	0.0125	0.0149	0.0172	0.0201	0.0216	0.0272

**Table S3.** Computed bandgap (PBE) of the MoSe<sub>2</sub>/MoS<sub>2</sub> heterobilayer with and without geometric optimization under the electric field.

Electric field (V/ Å)	0.1	0.2	0.3	0.4	0.5
Direct gap	0.67	0.58	0.49	0.42	0.34
Indirect gap	0.70	0.65	0.59	0.54	0.49
Direct gap after geometric optimization	0.67	0.58	0.49	0.43	0.31
Indirect gap after geometric optimization	0.70	0.65	0.59	0.55	0.47